ARTICLES
PUBLISHED ONLINE: 22 JANUARY 2012 | DOI: 10.1038/NPHYS2196
nature physics

Optical cavity cooling of mechanical modes of a semiconductor nanomembrane

K. Usami[1], A. Naesby[1], T. Bagci[1], B. Melholt Nielsen[1], J. Liu[1,2], S. Stobbe[1], P. Lodahl[1] and E. S. Polzik[1]*

Mechanical oscillators can be optically cooled using a technique known as optical-cavity back-action. Cooling of composite metal–semiconductor mirrors, dielectric mirrors and dielectric membranes has been demonstrated. Here we report cavity cooling of mechanical modes in a high-quality-factor and optically active semiconductor nanomembrane. The cooling is a result of electron–hole generation by cavity photons. Consequently, the cooling factor depends on the optical wavelength, varies drastically in the vicinity of the semiconductor bandgap, and follows the excitonic absorption behaviour. The resultant photo-induced rigidity is large and a mode temperature cooled from room temperature down to 4 K is realized with 50 μW of light and a cavity finesse of just 10. Thermal stress due to non-radiative relaxation of the electron–hole pairs is the primary cause of the cooling. We also analyse an alternative cooling mechanism that is a result of electronic stress via the deformation potential, and outline future directions for cavity optomechanics with optically active semiconductors.

The first experimental demonstration of cavity back-action cooling of mechanical modes used photothermal (bolometric) force with a low-finesse cavity made of a gold-coated silicon microlever and a fibre surface[1,2]. Radiation pressure on dielectric mirrors[3–6] and membranes[7,8] has recently become the mainstream approach[9–11] for cooling mechanical modes and culminated in reaching the quantum ground state[12,13].

Applying the cavity cooling method to optically active semiconductors[14–17] offers interesting prospects because the internal semiconductor bandgap and the externally introduced cavity resonance are intertwined. For instance, the strong deformation potential coupling between the mechanical and electronic degrees of freedom in semiconductors[18] could be exploited for cavity optomechanics. Investigation of cavity cooling with semiconductors could also shed new light on the optical refrigeration scheme to be realized with semiconductors[19]. Semiconductor devices with engineered electronic and photonic band structures have enabled, for example, strongly enhanced light–matter interactions for quantum photonics applications[20,21]. Studying the interaction between the laser-cooled mechanical modes and the engineered internal degrees of freedom could provide new insights into electronics, photonics and optoelectronics applications.

Driven by these prospects we have manufactured a 160-nm-thick crystalline gallium arsenide (GaAs) membrane[22]. Here we report the first experimental realization of cavity cooling of mechanical modes in the semiconductor nanomembrane with the cooling mechanism involving both the internal electronic degrees of freedom and the externally tunable cavity resonance. The experimental set-up and the structure of the fabricated GaAs membrane are shown in Fig. 1. A detailed account of the fabrication process of the nanomembranes and their mechanical properties can be found in ref. 22.

With the set-up shown in Fig. 1a the Brownian motion of the membrane can be measured[23] either by looking at the cavity field transmission or by using an external probe light using a beam deflection method. Figure 2a shows the calibrated power spectra of the Brownian peak for the mechanical resonances (the (2, 1)-mode) taken by the cavity transmission for different cavity input powers where the wavelength of the laser is 870 nm. The area of the peak, which is proportional to the effective mode temperature $T_{\rm eff}$ (refs 1,2), clearly becomes smaller as the cavity input power increases, showing the cooling effect. Figure 2b shows the results of a mechanical ringdown taken by the beam deflection method, demonstrating that the damping rate is enhanced by the cavity field and is proportional to the cavity input power, as is expected from the optomechanically modified damping model[1,2]. Also shown is the frequency shift as a result of the cavity field. The cooling can be observed only when the frequency of the cavity resonance $\Omega_{\rm C}/2\pi$ is detuned to the red from the frequency of the laser $\Omega_{\rm L}/2\pi$, that is, $\Omega_{\rm C} < \Omega_{\rm L}$, as opposed to the case of cavity cooling via radiation pressure[9–11]. The optomechanical instability[9–11] sets in (that is, the mechanical decay rate becomes negative) when $\Omega_{\rm C} > \Omega_{\rm L}$, even for the cavity input power as low as 5 μW.

The optomechanically modified mechanical resonance frequency $\omega_{\rm eff}/2\pi$ and the effective damping rate $\Gamma_{\rm eff}$ are expressed as functions of a photo-induced force $F_{\rm ph}$ and a relevant time lag τ (refs 1,2), that is, $\omega_{\rm eff}^2 = \omega_0^2(1-(1/(1+\omega_0^2\tau^2))(\nabla F_{\rm ph}/m\omega_0^2))$ and $\Gamma_{\rm eff} = \Gamma_0(1+Q_0(\omega_0\tau/(1+\omega_0^2\tau^2))(\nabla F_{\rm ph}/m\omega_0^2))$, respectively, with the motional mass m, the intrinsic mechanical decay rate Γ_0, frequency $\omega_0/2\pi$ and quality factor $Q_0 \equiv \omega_0/\Gamma_0$. $\nabla F_{\rm ph}(z)$ is the photo-induced rigidity, that is, the spatial derivative of $F_{\rm ph}$. The effective temperature can then be defined as $T_{\rm eff} = T/(\Gamma_{\rm eff}/\Gamma_0)$ (ref. 2). The ratio of the highest effective damping rate $\Gamma_{\rm eff}$ to the extrapolated intrinsic damping rate Γ_0 thus gives the maximum cooling factor $\Gamma_{\rm eff}/\Gamma_0$. In our setting $\Gamma_{\rm eff}$ is limited by the onset of an instability of the system caused by the static photothermal deformation of the membrane (see Supplementary Information), which can be observed when the cavity input power exceeds around 50 μW on the cooling side ($\Omega_{\rm C} < \Omega_{\rm L}$).

In Fig. 2c we compare the calibrated spectra with the ringdown results performed under the same conditions. For comparison both results are converted into a temperature scale, where the mode overlap between the cavity beam and the mechanical mode[24] is taken into account in converting the displacement results into the mode temperature. For the ringdown the mode temperature

[1]Niels Bohr Institute, University of Copenhagen, Blegdamsvej 17, DK-2100 Copenhagen, Denmark, [2]DTU Fotonik, Department of Photonics Engineering, Technical University of Denmark, Ørsteds Plads 343, DK-2800 Kgs. Lyngby, Denmark. *e-mail: polzik@nbi.dk.

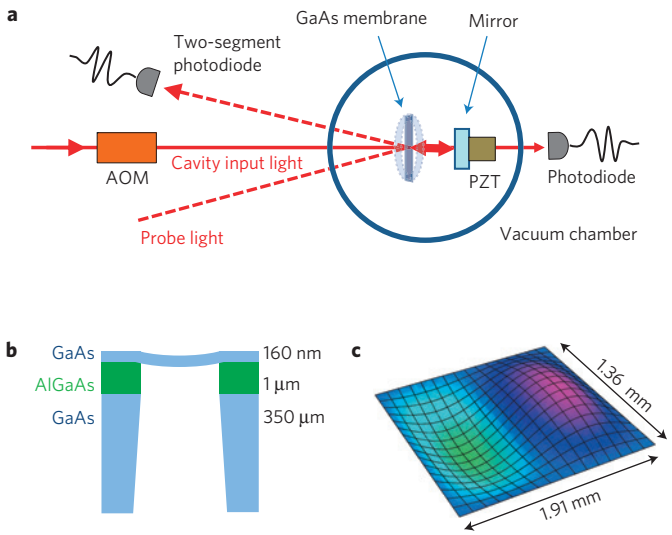

Figure 1 | Experimental set-up and structure of the fabricated GaAs membrane. a, Sketch of the experimental set-up. A dielectric concave mirror with a reflectivity of 96% and a membrane with a reflectivity of roughly 62% form a hemispherical cavity with a measured finesse of about 10 (essentially constant in the range of laser wavelength from 810 nm to 884 nm). The cavity is placed in a vacuum chamber maintained at 10^{-5} Pa. The cavity length (~29 mm) can be varied by means of a piezoelectric transducer (PZT) attached to the end mirror. A Ti:sapphire laser (810 nm–880 nm) is used as a cavity input for both cooling and inducing mechanical oscillations (the beam spot radius at the membrane is about 80 μm) by modulating its intensity by means of an acousto-optic modulator (AOM). A diode laser (975 nm) is used to probe the membrane oscillations using a beam deflection method with a two-segment photodiode. **b**, Cross-section of the 160-nm-thick suspended GaAs membrane (not to scale). The membrane is intrinsically bent slightly (about 0.1% of the lateral size); the bending shown in the figure is grossly exaggerated. **c**, Lateral dimensions of the membrane. The mechanical mode shown is the (2, 1)-mode.

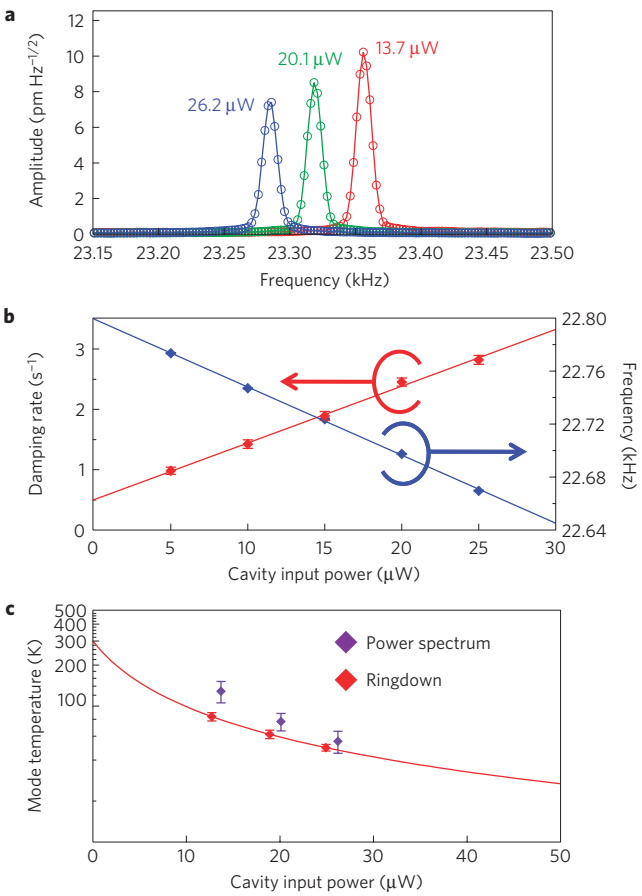

Figure 2 | Cooling results. a, Calibrated power spectra (resolution bandwidth: 10 Hz) of the Brownian peaks ((2, 1)-mode) for different cavity input powers (the wavelength of the laser is 870 nm). **b**, Results of the mechanical ringdown. Red and blue diamonds represent the measured damping rate and the frequency, respectively. Each point is the average of five identical measurements and the error bars correspond to one standard deviation; the lines are their least-square linear fits. **c**, A comparison of the mode temperatures deduced from the calibrated power spectrum (purple points) and those from ringdown results performed under the same conditions (red points). Each point is the average of five identical measurements and the error bars correspond to one standard deviation; the red line is produced by the least-square linear fit to the inverse of the ringdown time.

in the absence of the cavity field is assumed to be 300 K. The mode temperatures obtained with these two methods agree well with each other. The heating of the nanomembrane due to photo-absorption is thus not significant for the range of cavity input power we could examine ($\lesssim$50 μW). For the (2, 1)-mode, from the slope in Fig. 2b, the cooling factor for 50-μW cavity input is found to be about 10. For the (4, 3)-mode, which has the highest mechanical Q_0 of 2.3×10^6 (ref. 22), the cooling factor is about 75 (see Supplementary Information), meaning that the effective temperature of this particular mode is reduced down to 4 K from room temperature (when assuming the heating is insignificant for this mode as well).

A special feature of the cooling is the dependence of the cooling factor on the photon energy (wavelength) of the cavity field. The measured cooling factors for a cavity input power of 50 μW with photon energy in the range from $E = 1.53$ eV (810 nm) down to 1.40 eV (884 nm) across the bandgap $E_g = 1.424$ eV (870.8 nm) are shown in Fig. 3. The cooling factor is essentially constant from $E \gg E_g$ to $E \sim E_g$, then varies drastically and ceases to have an effect when $E < E_g - k_B T$ (k_B is the Boltzmann constant and $k_B T \sim 26$ meV at room temperature), which basically follows the excitonic absorption spectrum[25]. A sharper excitonic absorption edge can be expected at lower temperature, which is interesting from the viewpoint of the proposed single-mirror Doppler optomechanics[26]. The origin of the small bump(s) in the cooling factor around the bandgap E_g is unknown at present and requires further investigation.

The second special feature of the cooling is its dependence on the cavity detuning (Fig. 4). Because of the finite thickness of the membrane ($l = 160$ nm) the system consisting of the semi-transparent membrane and the mirror should be treated as a coupled two-cavity system formed by the two surfaces of the membrane and the end mirror (Supplementary Information). Figure 4a shows the calculated power transmission, reflection and absorption probabilities of the coupled cavity for an photon of wavelength 870 nm. The reflection and absorption exhibit shifted asymmetric resonances with respect to the cavity detuning because of interference effects inside the membrane. The maximum probability of the absorption reaches more than 50% even though the single-pass absorption probability is just 8%. The intra-membrane photon number n_{mem} shows the same behaviour as the absorption (see the red solid line in Fig. 4b). The photo-induced force $F_{ph}(z)$ is presumably proportional to the number of photons in the membrane, n_{mem}. This coupled cavity picture (Supplementary Information) explains the observed abnormal dependence of the cooling factor on the cavity detuning as $\Gamma_{eff}/\Gamma_0 - 1 \propto \nabla F_{ph} \propto \nabla n_{mem}$,

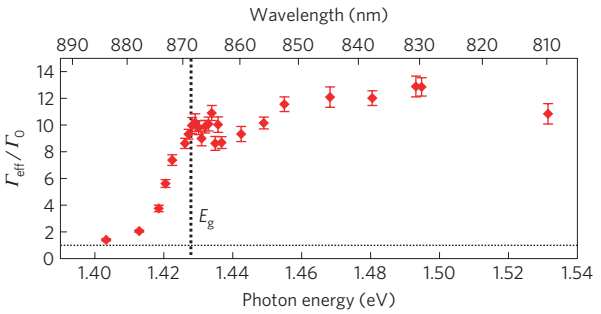

Figure 3 | Dependence of the cooling factor on the photon energy (wavelength) of the cavity field. Each point corresponds to an average cooling factor Γ_{eff}/Γ_0 from five identical ringdown measurements and the error bars correspond to one standard deviation. The black dotted vertical line indicates the GaAs bandgap energy $E_g = 1.424$ eV (870.8 nm) and the black dotted horizontal line represents a cooling factor equal to one, that is, no cooling.

where ∇n_{mem} is the spatial derivative of n_{mem} with respect to the membrane displacement, as shown in Fig. 4b.

The mechanical resonance frequency $\omega_{eff}/2\pi$ shown in Fig. 4c, on the other hand, shows a different behaviour from the model of dynamic optomechanical back-action[1,2]. In the model[1,2], the frequency shift stems only from the dynamic contribution of the photo-induced force, but in general the static part of F_{ph} not only leads to a static displacement of the membrane (which is indeed responsible for the aforementioned instability of the system (Supplementary Information)) but also to a static spring constant change due to the change of the tensile stress of the membrane σ_T (this is especially true for low tensile stress membranes). This frequency shift is induced by the local temperature rise δT at the membrane due to the photon absorption, which is proportional to the intra-membrane photon number n_{mem}. This n_{mem}-dependence of ω_{eff} (instead of a ∇n_{mem}-dependence) is shown in Fig. 4c.

Several mechanisms could be responsible for this efficient cooling. The radiation pressure mechanism[3–6] can be ruled out by the wavelength dependence (Fig. 3) and by the fact that its effect is negligible with our low cavity finesse. The wavelength dependence in Fig. 3 suggests that electron–hole pair excitation is responsible for the optomechanical force. The electron–hole pair excitation and relaxation can induce both electronic and thermal pressure on the membrane[27,28]. The membrane is intrinsically bent slightly (about 0.1% of the lateral size) towards the end mirror, from which the membrane oscillates with a lesser amplitude (such a bending is probably generic for large membranes; the direction of the bending may change from sample to sample). The growth of carriers inside the membrane (which is proportional to the intra-membrane photon number) due to the membrane motion (which is coupled to the cavity length) leads to further membrane deformation due to the electronic and thermal stress towards the end mirror, shrinking the cavity length. This provides the optomechanical coupling and explains why the cavity detuning corresponding to cooling in the present case is opposite to that for radiation pressure cooling.

The strengths of the electronic stress and the thermal stress can be compared in the following way[27,28]. The electronic stress per electron–hole pair is given by $\sigma_{el} = -B(dE_g/dp) \sim 8$ eV per unit volume (where $-B(dE_g/dp)$ is the hydrostatic deformation potential denoting the bandgap change due to the longitudinal strain $(-p/B)$, with p being the hydrostatic electronic pressure and B the bulk modulus) and short-lived, limited by the carrier lifetime. On the other hand, the thermal stress is given by $\sigma_{th} = -3B\beta(\eta E/C) \sim 0.8\eta E$ eV per unit volume, where β and C denote the thermal expansion coefficient and the heat capacity, respectively. The parameter η represents the conversion efficiency

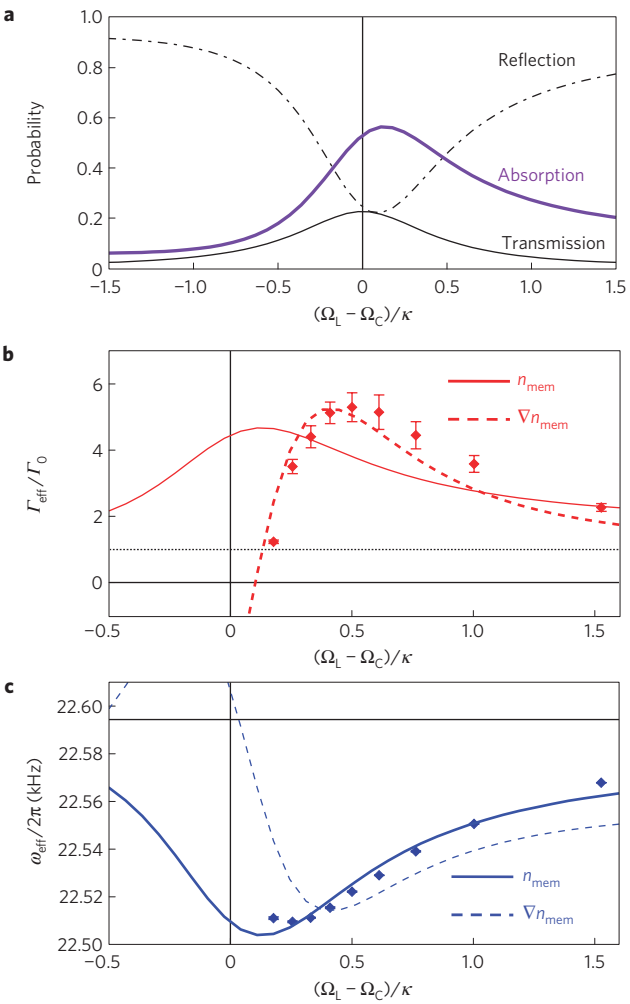

Figure 4 | Cavity detuning dependences. a, Calculated power transmission, reflection and absorption probabilities for the coupled cavity for an input photon with a wavelength of 870 nm. **b**, Dependence of the cooling factor Γ_{eff}/Γ_0 on cavity detuning. **c**, Dependence of the mechanical resonance frequency $\omega_{eff}/2\pi$ on cavity detuning. Both data are for the (2,1)-mode, where each point is the average of five identical measurements for an input power of 20 μW and the error bars correspond to one standard deviation. The cavity detuning is normalized to the cavity bandwidth κ. In Fig. 4a (Fig. 4b) the solid red (blue) line shows the best fits assuming Γ_{eff}/Γ_0 ($\omega_{eff}/2\pi$) follows n_{mem}; the dashed lines show those fits assuming they follow ∇n_{mem}. The black dotted horizontal line in **b** represents a cooling factor equal to one, that is, no cooling. The black solid horizontal line in **c** represents the estimated intrinsic mechanical frequency $\omega_0/2\pi = 22.594$ kHz.

from the absorbed photon energy E to heat (phonons) and runs from its maximum value of 1 (all photon energy E is converted into heat via non-radiative decay) to its minimum value $(E - E_g)/E$ (perfect radiative decay). From the mechanical resonance frequency change shown in Fig. 4c we could estimate that $\eta \sim 0.9$ for our sample.

Although $\sigma_{el} > \sigma_{th}$, the dominant of these two contributions is determined by the number of excited pairs and by their relaxation mechanism. To figure out the nature of the cooling mechanism we performed two complementary experiments (Supplementary Information) and confirmed that the thermal stress due to the non-radiative relaxation of the electron–hole pairs is the main mechanism of the cooling. The contribution of the electronic pressure to the cooling is negligibly small. From the formula for the

effective damping rate $\Gamma_{\rm eff}$ with the time lag τ equal to the thermal diffusion time $\tau_{\rm th} \sim 10$ ms (see Supplementary Information) we arrive at a very large photo-induced rigidity $\nabla F_{\rm ph} \sim 0.5\,{\rm N\,m^{-1}}$ for the (2, 1)-mode, where we use $m\omega_0^2 \sim 11\,{\rm N\,m^{-1}}$ with the motional mass of the membrane $m = 520$ ng. As $\nabla F_{\rm ph}$ scales linearly in cavity input power and quadratically in cavity finesse we can estimate $\nabla F_{\rm ph}$ for the other systems on the same footing. For the photothermal cooling with a metal-coated microlever in ref. 1, for instance, $\nabla F_{\rm ph} \sim 0.007\,{\rm N\,m^{-1}}$; a factor 70 times smaller. For the radiation pressure cooling the corresponding $\nabla F_{\rm ph}$ is significantly smaller (for example, $\nabla F_{\rm ph} = 0.5 \times 10^{-4}\,{\rm N\,m^{-1}}$; ref. 6).

To reach even lower temperatures we need to deal with the static photothermal deformation of the membrane (Supplementary Information), which limits the cooling at present. It is thus beneficial to exploit the electronic stress instead of the thermal stress. With the photon number absorbed per unit time being $\delta n_{\rm mem}$ the total electronic stress $\sigma_{\rm el}\delta n_{\rm mem}\tau_{\rm el}$ is smaller than the total thermal stress $\sigma_{\rm th}\delta n_{\rm mem}\tau_{\rm th}$ when the lifetime of the electronic pressure $\tau_{\rm el}$ is substantially shorter than that of the thermal stress $\tau_{\rm th}$. This is the reason why the thermal stress at present overwhelms the electronic stress ($\tau_{\rm el}/\tau_{\rm th} \leq 5 \times 10^{-9}$ in our situation). A quantum-well structure, for instance, could minimize the non-radiative surface recombination (thus minimize η) and maximize the radiative decay probability. If $\eta \sim (E - E_{\rm g})/E$, the ratio of electronic to thermal stress, $\sigma_{\rm el}/\sigma_{\rm th}$, can be as large as 320 with the photon energy $E = 1.46$ eV (852 nm) and further grows for smaller E; for $E \sim E_{\rm g}$ it diverges. Note that even in the worst case scenario, $\eta \sim 1$, the ratio $\sigma_{\rm el}/\sigma_{\rm th}$ is still around 7 for $E \sim E_{\rm g}$.

The characteristic delay time τ can be also engineered to realize electronic-stress-based cavity cooling. One promising way is to employ the so-called membrane-in-the-middle approach[7,8], where a GaAs membrane is inside a cavity of higher finesse than the current one, for which the wavelength of the laser is optimized to reduce absorptive loss due to the membrane for the cavity, but to keep the finite absorption for electron–hole pair generation. By doing so τ could be governed by the cavity lifetime $\tau_{\rm cav} = 1/\kappa$ instead of the generally short carrier lifetime $\tau_{\rm el} < 1$ ns, because the cascade nature of the decay processes leads to $\tau = \tau_{\rm cav} + \tau_{\rm el} \sim \tau_{\rm cav}$. Under these conditions an intriguing interplay between electronic stress cooling and radiation pressure cooling can be explored.

It is interesting to note that the thermal expansion coefficient β for GaAs vanishes at 12 K and 50 K (refs 29,30). At these temperatures the photothermal force in principle diminishes[16,17]. The instability due to the thermal deformation could thus be eliminated and the electronic force can play a major role in the cooling. The thermoelastic damping[31] can also be minimized and Q_0 can be maximized in this regard[30]. This temperature flexibility is in stark contrast to the standard photothermal approach that explicitly exploits β and for which the optimal operating temperature is fixed at the Debye peak of the thermoelastic damping[31].

By the membrane-in-the-middle approach, when starting from the 'magic' temperature 12 K, an estimate (Supplementary Information) suggests that the cooling with the electronic stress has a slightly better performance than that with the radiation pressure and that cooling close to the ground state can be feasible with a critically coupled cavity with a finesse of 3,000 and the cavity input power of 10 μW. The issue of whether the dissipative cooling approach could really lead to the ground-state cooling remains to be investigated, although there are relevant analyses on the photothermal cooling[32,33].

The cavity back-action cooling with optically active semiconductors proved to exhibit very rich physics because of their internal electronic degrees of freedom, which may open up a new panorama for cavity optomechanics. Conversely, the intricate quantum process involving electrons, phonons and photons in semiconductors could be explored by means of the strong optomechanical coupling described in this work.

Received 21 November 2010; accepted 2 December 2011; published online 22 January 2012

References

1. Hohberger Metzger, C. & Karrai, K. Cavity cooling of a microlever. *Nature* **432,** 1002–1005 (2004).
2. Metzger, C., Favero, I., Ortlieb, A. & Karrai, K. Optical self-cooling of a deformable Fabry–Perot cavity in the classical limit. *Phys. Rev. B* **78,** 035309 (2008).
3. Gigan, S. *et al.* Self-cooling of a micromirror by radiation-pressure. *Nature* **444,** 67–70 (2006).
4. Arcizet, O., Cohadon, P. F., Briant, T., Pinard, M. & Heidmann, A. Radiation pressure cooling and optomechanical instability of a micromirror. *Nature* **444,** 71–74 (2006).
5. Schliesser, A., Del'Haye, P., Nooshi, N., Vahala, K. J. & Kippenberg, T. J. Radiation pressure cooling of a micromechanical oscillator using dynamical backaction. *Phys. Rev. Lett.* **97,** 243905 (2006).
6. Corbitt, T. *et al.* An all-optical trap for a gram-scale mirror. *Phys. Rev. Lett.* **98,** 150802 (2007).
7. Thompson, J. D. *et al.* Strong dispersive coupling of a high-finesse cavity to a micromechanical membrane. *Nature* **452,** 72–75 (2008).
8. Wilson, D. J., Regal, C. A., Papp, S. B. & Kimble, H. J. Cavity optomechanics with stoichiometric SiN films. *Phys. Rev. Lett.* **103,** 207204 (2009).
9. Kippenberg, T. J. & Vahala, K. J. Cavity optomechanics: Back-action at the mesoscale. *Science* **321,** 1172–1176 (2008).
10. Favero, I. & Karrai, K. Optomechanics of deformable optical cavities. *Nature Photon.* **3,** 201–205 (2009).
11. Marquardt, F. & Girvin, S. M. Trend: Optomechanics. *Physics* **2,** 40 (2009).
12. Teufel, J. D. *et al.* Sideband cooling of micromechanical motion to the quantum ground state. *Nature* **475,** 359–363 (2011).
13. Chan, J. *et al.* Laser cooling of a nanomechanical oscillator into its quantum ground state. *Nature* **478,** 89–92 (2011).
14. Ding, L. *et al.* High frequency GaAs nano-optomechanical disk resonator. *Phys. Rev. Lett.* **105,** 263903 (2010).
15. Ding, L. *et al.* Wavelength-sized GaAs optomechanical resonators with gigahertz frequency. *Appl. Phys. Lett.* **98,** 113108 (2011).
16. Okamoto, H. *et al.* Vibration amplification, damping, and self-oscillations in micromechanical resonators induced by optomechanical coupling through carrier excitation. *Phys. Rev. Lett.* **106,** 036801 (2011).
17. Okamoto, H. *et al.* Carrier-mediated optomechanical coupling in GaAs cantilevers. *Phys. Rev. B* **84,** 014305 (2011).
18. Wilson-Rae, I., Zoller, P. & Imamoğlu, A. Laser cooling of a nanomechanical resonator mode to its quantum ground state. *Phys. Rev. Lett.* **92,** 075507 (2004).
19. Sheik-Bahae, M. & Epstein, R. I. Optical refrigeration. *Nature Photon.* **1,** 693–699 (2007).
20. Hennessy, K. *et al.* Quantum nature of a strongly coupled single quantum dot-cavity system. *Nature* **445,** 896–899 (2007).
21. Lund-Hansen, T. *et al.* Experimental realization of highly efficient broadband coupling of single quantum dots to a photonic crystal waveguide. *Phys. Rev. Lett.* **101,** 113903 (2008).
22. Liu, J. *et al.* High-Q optomechanical GaAs nanomembranes. *Appl. Phys. Lett.* **99,** 243102 (2011).
23. Tittonen, I. *et al.* Interferometric measurements of the position of a macroscopic body: Towards observation of quantum limits. *Phys. Rev. A* **59,** 1038–1044 (1999).
24. Gillespie, A. & Raab, F. Thermally excited vibrations of the mirrors of laser interferometer gravitational-wave detectors. *Phys. Rev. D* **52,** 577–585 (1995).
25. Fox, A. M. *Optical Properties of Solids* (Oxford Univ. Press, 2001).
26. Karrai, K., Favero, I. & Metzger, C. Doppler optomechanics of a photonic crystal. *Phys. Rev. Lett.* **100,** 240801 (2008).
27. Thomsen, C., Grahn, H. T., Maris, H. J. & Tauc, J. Surface generation and detection of phonon by picosecond light pulses. *Phys. Rev. B* **34,** 4129–4138 (1986).
28. Matsuda, O., Tachizaki, T., Fukui, T., Baumberg, J. J. & Wright, O. B. Acoustic phonon generation and detection in GaAs/$Al_{0.3}Ga_{0.7}$As quantum wells with picosecond laser pulses. *Phys. Rev. B* **71,** 115330 (2005).
29. Sparks, P. W. & Swenson, C. A. Thermal expansions from 2 to 40° K of Ge, Si, and four III–V compounds. *Phys. Rev.* **163,** 779–790 (1967).
30. Okamoto, H., Ito, D., Onomitsu, K. & Yamaguchi, H. Thermoelastic damping in GaAs micromechanical resonators. *Phys. Status Solidi C* **5,** 2920–2922 (2008).
31. Lifshitz, R. & Roukes, M. L. Thermoelastic damping in micro- and nanomechanical systems. *Phys. Rev. B* **61,** 5600–5609 (2000).
32. Restrepo, J., Gabelli, J., Ciuti, C. & Favero, I. Classical and quantum theory of photothermal cavity cooling of a mechanical oscillator. *C. R. Phys.* **12,** 860–870 (2011).

33. De Liberato, S., Lambert, N. & Nori, F. Quantum noise in photothermal cooling. *Phys. Rev. A* **83,** 033809 (2011).

Acknowledgements

We thank J. Appel, A. Grodecka-Grad, K. Hammerer, A. Imamoğlu, H. J. Kimble, J. H. Müller, H. Okamoto, S. Schmid, J. M. Taylor, D. J. Wilson and A. Xuereb for discussions. This work was supported by the Japan Science and Technology Agency (JST), the Japan Society for the Promotion of Science (JSPS), the EU Project Q-ESSENCE, the Danish National Research Foundation Center for Quantum Optics (QUANTOP), the Danish Council for Independent Research (Technology and Production Science and Natural Science) and the DARPA QuASAR program.

Author contributions

K.U., B.M.N. and E.S.P. designed the experiment. K.U., A.N. and T.B. worked on data collection and analysis. J.L. and S.S. fabricated the GaAs membranes. P.L. and E.S.P. planned and supervised the study. K.U. and E.S.P. wrote the manuscript. All authors discussed the results and commented on the manuscript.

Additional information

The authors declare no competing financial interests. Supplementary information accompanies this paper on www.nature.com/naturephysics. Reprints and permissions information is available online at http://www.nature.com/reprints. Correspondence and requests for materials should be addressed to E.S.P.